Title

Simplified Green-Ampt Model, Imbibition-Based Estimates of Permeability, and Implications for Leak-off in Hydraulic Fracturing

Journal

Water Resources Research, 56(4)

ISSN

0043-1397

Author

Tokunaga, Tetsu K

Publication Date

2020-04-01

DOI

10.1029/2019wr026919

Peer reviewed

Simplified Green-Ampt model, imbibition-based estimates of permeability, and implications for leak-off in hydraulic fracturing

Tetsu K. Tokunaga[1*]

[1]Energy Geosciences Division, Lawrence Berkeley National Laboratory, Berkeley, CA, USA

*Corresponding author: Tetsu K. Tokunaga (tktokunaga@lbl.gov)

Key Points:

- The capillary pressure associated with the imbibition front can be approximated as a power function of permeability
- Scaling the wetting front capillary pressure to the permeability reduces uncertainty in the Green and Ampt imbibition equation
- A new correlation was developed to estimate permeabilities based on imbibition measurements

Abstract

Predicting water imbibition into porous materials is important in a wide variety of fields, and hydraulic fracturing of low permeability hydrocarbon reservoirs has emerged as an application that is imposing a large water footprint. Reliable predictions of imbibition are needed to better manage water use, yet are challenging because of uncertainties in both the permeability and capillary pressure driving force. Here, this uncertainty is reduced through evaluating correlations between the permeability and the effective capillary pressure associated with the wetting front, $P_{c,f}$. These correlations allow elimination of $P_{c,f}$ from the Green and Ampt equation, and concentrates all uncertainties in fluxes on the effective permeability k. Over a wide range of k and porosities n, imbibition scales approximately with $k^{1/3}$. Although Leverett $k^{1/4}$ scaling for predicting $P_{c,f}$ is shown to be inferior when tested with data spanning a wide range of n, it nevertheless predicted imbibition fairly well. From simple imbibition measurements, both the empirical and Leverett scaling approaches allow estimates of k that have root mean-square deviations of about 1 order of magnitude relative to measurements that ranged over 10 orders of magnitude in k.

1 Introduction

Water imbibition into porous media has a long history of investigation, beginning over a century ago in agriculture (Bell & Cameron, 1906; Green &

Ampt, 1911), and receiving subsequent studies in soil physics and other fields including materials science, petroleum engineering, and nanoscience (Leech et al., 2008; Mason & Morrow, 2013; Mattax & Kyte, 1962; Morrow & Mason, 2001; Philip, 1957a; Stukan, Ligneul, Crawshaw, & Boek, 2010; Tas, Haneveld, Jansen, Elwenspoek, & van den Berg, 2004; Washburn, 1921). The wide range of materials (soils, rocks, cements, ceramics) and fluids (water, oil, gas) involved in different imbibition processes has motivated the development of a variety of scaling analyses for providing unified predictions of immiscible displacement processes (Cai, Perfect, Cheng, & Hu, 2014; Leverett, 1941; Miller & Miller, 1956; Morrow & Mason, 2001; Philip, 1957a; Rapoport, 1955; Schmid & Geiger, 2012, 2013). In recent decades, hydraulic fracturing of unconventional gas reservoirs has emerged as a technology that consumes vast quantities of water as a consequence of imbibition into low permeability formations. Development of a typical horizontal well requires injection of about a million gallons of water, and most of this water remains in the reservoir where it can restrict production of hydrocarbon fluids (Agrawal & Sharma, 2013; Birdsell, Rajaram, & Lackey, 2015; Makhanov, Habibi, Dehghanpour, & Kuru, 2014; Zhou, Abass, Li, & Teklu, 2016). Thus, hydraulic fracturing of low permeability reservoirs constitutes an activity where imbibition is important to predict on an industrial scale. Indeed, the continued growth in water consumption for hydraulic fracturing (Kondash, Lauer, & Vengosh, 2018) combined with growing demands on water resources (Rosa, Rulli, Davis, & D'Odorico, 2018) warrants better understanding on how water is lost within reservoirs. Such understanding could provide part of the foundation for reducing the amounts of water used during reservoir stimulation.

The large volumes of water consumed for hydraulic fracturing of low permeability reservoirs and the immiscibility of water-based fracturing fluids with gas motivates the need to estimate the propagation of wetted zones from fractures into the unsaturated matrix (Figure 1). The early period of fluid injection and subsequent well shut-in is particularly important to understand because it is associated with the highest rates of water loss into reservoir rock. This initial period may be most amenable to simplified analysis because imbibition is presumably closest to being one-dimensional, advancing nominally orthogonally from fractures and microfractures into adjacent matrix rock. The laminated structure of shales can cause significant anisotropy in k (Armitage et al., 2011; Gensterblum et al., 2015; Roychaudhuri, Tsotsis, & Jessen, 2013), such that wetting front advance along bedding planes is expected to progress much more rapidly than across bedding planes (Figure 1d). Nevertheless, flow is approximately locally one-dimensional during times when imbibition distances are short. In comparison to the general problem of immiscible fluid displacement, water imbibition into initially gas-filled porous media is further simplified because the of relatively low viscosity of the native gas phase.

The simplifications allowed by the locally one-dimensional geometry and by the large viscosity contrast justify the application of the Green and

Ampt (GA) model for describing the early phase of hydraulic fracturing fluid distribution in unconventional reservoirs. It should be noted that although hydraulic fracturing fluids generally have complex rheology, Newtonian behavior will be assumed for flow through the matrix pores because the range of shear rates is limited by the low k of shale. The novel aspect of the analysis developed here is associated with evaluating the GA model's wetting front capillary pressure, $P_{c,f}$, based on scaling the matrix permeability k. It will be shown that by correlating $P_{c,f}$ with k, a simpler expression for wetting fluid imbibition is obtained, with potential reduction in uncertainty associated with imbibition volumes. The analyses will also show that simple imbibition measurements can be used to estimated k to within about an order of magnitude, in materials spanning over 10 orders of magnitude in k. These advantages are expected to be broadly applicable to interpreting early stages of imbibition, and example calculations for hydraulic fracturing are provided.

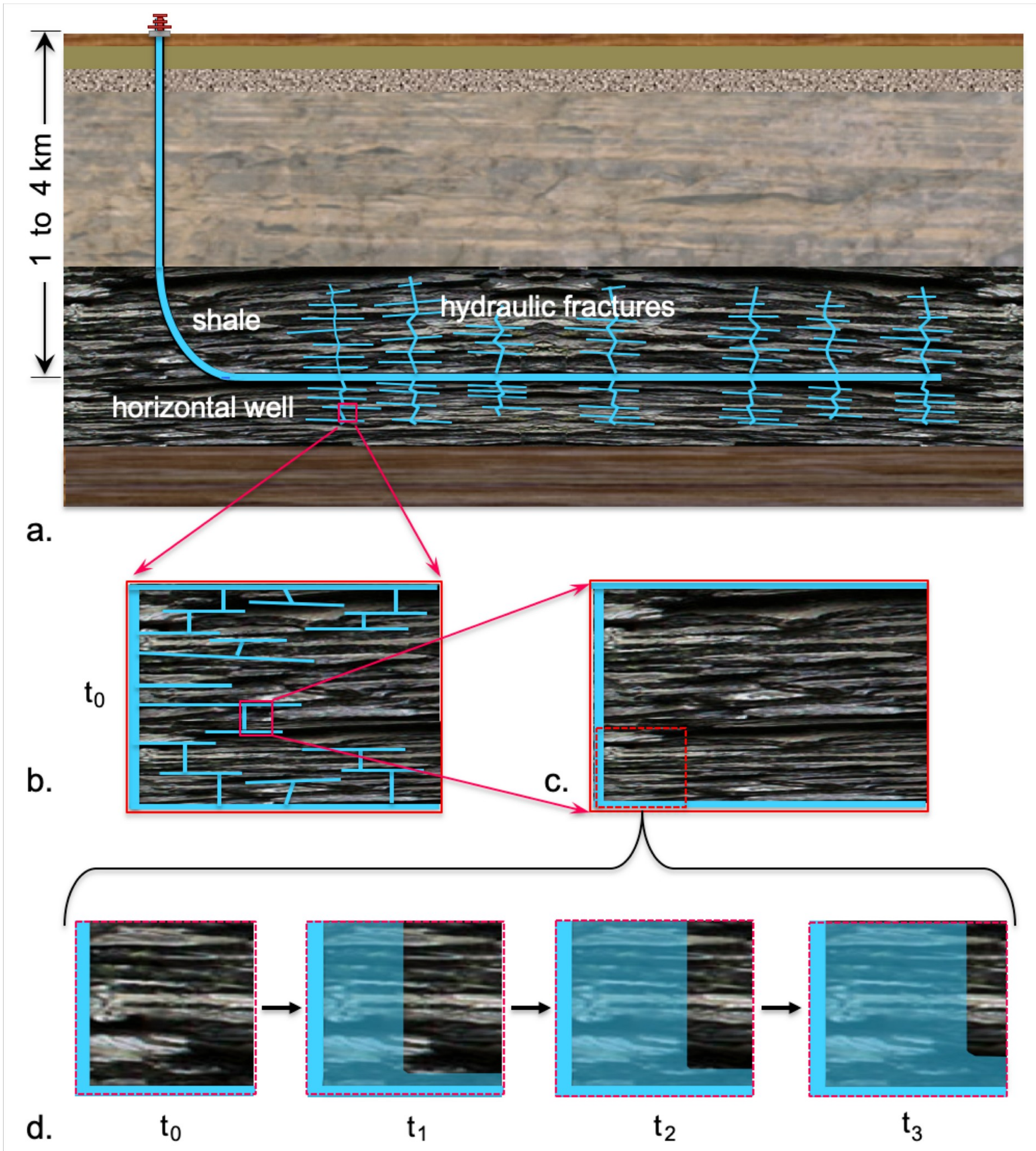

Figure 1. Conceptual model of early stages of water imbibition from hydraulic fractures into shale matrix. **a.** Distribution of water in vertical hydraulic fractures from perforated horizontal well, filling connected natural and stimulated horizontal fractures along shale bedding planes. **b.** Local distribution of water-filled microfractures immediately after fluid injection (time-zero). **c.** Representative local volume bounded by water-filled horizontal and vertical microfractures. **d.** Time evolution of wetted zones advancing into matrix with anisotropic *k*, along and transverse to bedding planes.

2 The Green & Ampt model, and the sorptivity

The profile of water advancing into an unsaturated porous medium is complex because of the saturation-dependence of the hydraulic conductivity, resulting in its nonlinear behavior (Richards, 1931). However, the earliest models describing capillary imbibition in porous media (Bell & Cameron, 1906; Green & Ampt, 1911) employed two simplifications to represent the basic physical process: treatment of the wetting profile as one having a constant saturation up to the wetting front, and the assignment of a distinct capillary pressure head to the wetting front, $h_{c,f}$. With these approximations, the instantaneous Darcy flux is equated to the product of the effective hydraulic conductivity K_e of the approximately uniformly wet transmission zone (Bodman & Coleman, 1944) times the hydraulic head gradient. Furthermore, when the gradient in gravitational head is negligible relative to that of the capillary pressure head, the latter gradient largely determines flow. This condition applies at short times for nearly all porous media, and over longer times in unsaturated shales because of very high P_c associated with wetting and draining shale matrix pores (Busch & Amann-Hildenbrand, 2013; Chenevert, 1970; Donnelly et al., 2016; Makhanov et al., 2014; Schmitt, Forsans, & Santarelli, 1994; Tokunaga et al., 2017; Yang et al., 2017). Thus, the hydraulic gradient is effectively equal to the difference between the pressure head at the inlet ($h_{c,0}$, here being the fracture-matrix interface) and at the wetting front, divided by the wetting length (distance of wetting front penetration, L). With the volumetric water content increased by $\Delta\theta$ within the wetted zone, the Darcy flux entering the matrix in the GA model depends on time t as

$$\frac{dL}{dt}=\frac{K}{\Delta\theta}\frac{h_{c,f}-h_{c,0}}{L} \tag{1}$$

which integrates to

$$L(t)=\sqrt{\frac{2K}{\Delta\theta}\left(h_{c,f}-h_{c,0}\right)}\sqrt{t} \tag{2}$$

In terms of permeability k, water viscosity η, and capillary pressure P_c, this relation is

$$L(t)=\sqrt{\frac{2k}{\eta\Delta\theta}\left(P_{c,f}-P_{c,0}\right)}\sqrt{t} \tag{3a}$$

In the GA model, the volumetric water flux per unit area $I(t)=\Delta\theta L(t)$, thus

$$I(t)=\sqrt{\frac{2\triangle\theta k}{\eta}\left(P_{c,f}-P_{c,0}\right)}\sqrt{t} \tag{3b}$$

which is equivalent to Equation (8) in Handy, who was apparently unaware of the much earlier GA model (Handy, 1960). Thus, the wetting front and cumulative imbibition advance with the square-root of time because the instantaneous flux is inversely proportional to the wetted distance. This basic relation due to Green and Ampt has been extended through a number of modifications (Ma, Zhang, Lu, Wu, & Wang, 2015; Mein & Larson, 1973; Selker & Assouline, 2017). It is important to note that uncertainties are associated with both k and $P_{c,f}$ in Equation (3), and because these parameters are multiplied, predictions of imbibition and L have significant uncertainty.

Before further developing the GA analysis, it is worth recognizing two factors that can limit its range of applicability: heterogeneity and structural stability. When k varies significantly along the imbibition length, a spatially averaged k will not generally be reliable for predicting water uptake. Similarly, when the porous matrix changes with time, k becomes time-dependent and deviations from the GA analysis are expected. This latter limitation is encountered when the influence of clay swelling is important, and thus applies to some soils and shales. Indeed, swelling during water imbibition can destroy the structural integrity of unconfined shale cores that contain high fractions of smectite (Chenevert, 1970) or even illite clays (Dehghanpour, Lan, Saeed, Fei, & Qi, 2013). Such samples are susceptible to disaggregation, especially along bedding planes, because they previously existed under very high confining stresses. The following developments apply on materials where k is relatively homogeneous and stable.

A new extension of the GA approach will be developed to eliminate the need for the P_c terms, thereby potentially reducing uncertainty associated with imbibition calculations. $P_{c,f}$ has commonly been evaluated as

$$P_{c,f}=\int_0^{P_{c,l}} k_r \, dP_c \tag{4}$$

where k_r is the relative permeability and $P_{c,l}$ is the arbitrary upper limit of integration where k_r becomes negligible (Bouwer, 1964; Neuman, 1976). However, given that $k_r(P_c)$ is seldom measured, determining $P_{c,f}$ is commonly challenging. For example, numerical simulations of infiltration for a variety of soils at different initial water saturations yielded ratios of $P_{c,f}$ relative to the gas (air) entry P_c (denoted $P_{c,g}$ here) that varied from 0.232 up to 1.369 (Ma et al., 2015). This wide range underscores the need to reduce uncertainty in $P_{c,f}$.

The first step in this analysis is to assume that $P_{c,f}$ can be approximated as a simple power function of k through

$$P_{c,f} = j_2 k^{\alpha} \tag{5}$$

with the parameters j_2 and α dependent on the selected scaling approaches described shortly. For later scaling comparisons, it will be useful to express $P_{c,0}$ as $bP_{c,f}$, with $b < 0$ when the water source is under positive pressure (boundary conditions for shut-in hydraulic fractures and ponded soils). With these relations, the cumulative imbibition becomes

$$I(t)=\left[\left(\frac{2 j_2 \triangle\theta}{\eta}(1-b)\right)^{1/2} k^{(1+\alpha)/2}\right] t^{1/2} \tag{6}$$

The square-root of time proportionality of infiltration under negligible influences of gravity and $b = 0$ is commonly termed the sorptivity S (Philip, 1957a)

$$I(t)=S\sqrt{t} \tag{7}$$

which encompasses the influences of porous media properties, fluid properties, and the pressure gradient. Thus, with eq. 5 and 6, the sorptivity is

$$S=\left(\frac{2 j_2 \triangle\theta}{\eta}\right)^{1/2} k^{(1+\alpha)/2} \tag{8}$$

In the following developments, the initial moisture contents of the porous media are assumed to be close to zero, recognizing that imbibition rates are slower under higher initial saturations. For example, at 40% initial saturation, values of S are about 25% lower relative to initially dry conditions (Philip, 1957b; Stewart, Rupp, Abou Najm, & Selker, 2013).

3 Estimating permeability from sorptivity

Although several relations have been developed for calculating k from S, most require information on unsaturated hydraulic properties (Dirksen, 1979; Stewart et al., 2013; White & Perroux, 1987). The simplicity of imbibition experiments relative to measurements of k motivates interest in developing estimates of k based solely on S. Previously, a model for predicting wetting front advance (Kao & Hunt, 1996) was used to develop one simple k – S relation (Tokunaga & Wan, 2001b)

$$k=\left(\frac{\eta}{\sigma}\right)^2\left(\frac{S}{B\,\Delta\theta}\right)^4 \tag{9a}$$

where σ is the water-gas interfacial tension and B is an empirical factor about equal to 0.5. Based on the GA model and eq. 8,

$$k=\left(\frac{\eta}{2\,j_2\,\triangle\,\theta}\right)^{\left(\frac{1}{1+\alpha}\right)} S^{\left(\frac{2}{1+\alpha}\right)} \tag{9b}$$

As part of this study, two alternative k – S relations will be developed based on approaches that provide different values of α and j_2 in eq. 9b.

With $P_{c,0}$ = 0, the first new k – S relation is developed based on applying Leverett scaling to eq. 9b. Using $P_{c,f}$ and approximating the porosity n with $\Delta\theta$, the Leverett J function is

$$J=\frac{P_{c,f}}{\sigma}\left(\frac{k}{\Delta\theta}\right)^{1/2} \tag{10}$$

and

$$P_{c,f}=J\sigma\left(\frac{\Delta\theta}{k}\right)^{1/2} \tag{11}$$

Thus, under Leverett scaling, α = -1/2, our generic $j=J\sigma\,\Delta\theta^{1/2}$, and eq. 9b becomes

$$k=\left(\frac{\eta}{2\,\sigma J}\right)^{2}\left(\triangle\,\theta\right)^{-3} S^{4} \tag{12}$$

a result that is similar to eq. 9a, except for the $\Delta\theta$ term. The second new k – S relation will be obtained after identifying the α parameter that best fits the compiled $P_{c,g}$–k data, and applying it in eq. 9b.

Note the above approaches for estimating k do not account for influences of different types of pore network geometries. Shale pore networks are not scaled down versions of those in sandstones, much less those in unconsolidated granular media. For unconsolidated porous materials, analyses that include grain aspect ratios (Katagiri, Saomoto, & Utsuno, 2015) could lead to improved predictions. However, refinement of predictions of k based on pore structure information are beyond the scope of this work. This present study is limited to evaluating correlations between S and k so that the latter can be easily estimated from simple measurements of imbibition rates.

4 Methods

In order to develop predictions of imbibition that are simpler than the original GA model while being based on measurements of P_c, k, and $k_r(P_c)$, the correlation between $P_{c,g}$ and k is first determined. Then, literature data were assembled to determine correlation between $P_{c,g}$ and $P_{c,f}$, with the latter calculated according to eq. 4. This allows determination of the desired $P_{c,f}$–k correlation, and the best fit α value. An earlier data set on $P_{c,g}$ and k for air-water systems (Tokunaga & Wan, 2001a) was expanded with additional values, especially for consolidated materials. Following that earlier study, drainage resulting in 97% water saturation was used as the criterion for assigning $P_{c,g}$ values. Data from air-water measurements were scaled for methane-water for purposes of estimating fracturing fluid imbibition in reservoirs. The adjustment needed to address reservoir conditions was obtained through the ratio of the interfacial tension of air-water at room temperature and pressure (72 mN/m), and the interfacial tension of gas (methane)-water at reservoir temperatures and pressures. These latter conditions were taken as 70 ˚C and 20 MPa, for which the interfacial tension of methane-water is about 50 mM/m (Sachs & Meyn, 1995; Schmidt, Folas, & B., 2007). Thus, the ratio of interfacial tensions of about 0.70 was used to adjust capillary influences from measurements obtained under ambient (air-water) to elevated temperatures and pressures for methane-water. A very large data set on low permeability sandstones (Byrnes, Cluff, & Webb, 2009) was also added, with its mercury (Hg) intrusion P_c values scaled to methane-water assuming 485 mN/m for the Hg-gas interfacial tension (Giesche, 2006).

While a fairly large database was compiled for estimating $P_{c,g}$ based on k, estimates of $P_{c,f}$ values are needed in order to implify the GA imbibition equation. For this purpose, experimentally determined $k_r(P_c)$ relations available in the literature were integrated according to eq. 4, to calculate $P_{c,f}$. Finally, in order to test S-based predictions of k, literature values of k and S were compiled from sources where both parameters were experimentally determined on the same materials.

5 Results

5.1 Predicting $P_{c,g}$ from permeability Literature data collected on $P_{c,g}$–k span 12 orders of magnitude in k, over 4 orders of magnitude in $P_{c,g}$, and have porosities ranging from 0.013 to 0.57 (Supporting Information, Table S1 and Table S2). The $P_{c,g}$ values associated with k are plotted in Figure 2, and tabulated in Supporting Information. Although there exists considerable scatter in this plot, the correlation between $P_{c,g}$ and k is described fairly well by a power function with $\alpha =$ -0.360

$$P_{c,g} = j_1 k^{\alpha} = \left(0.0754\, Pa\, m^{0.720}\right) k^{-0.360} \tag{13}$$

which has a root mean square deviation (rmsd) in *log* P_c of 0.705. The regression relation for k and methane breakthrough P_c reported by Busch and Amann-Hildenbrand has been added to this plot (Busch & Amann-Hildenbrand, 2013), and has nearly the same slope ($k^{-0.32}$) as our regression relation, but its predicted P_c values run about a factor of about 3.6 lower than ours. The offset between these correlations is consistent with lower P_c values associated with percolation breakthrough of the nonwetting phase relative to water drainage to 97% saturation. The considerable scatter in the data is reasonable, given the wide range of porosities, pore structures, and wettabilities expected in this very wide range of materials. It should be noted that rather than being -0.360, the exponent for k in Equation 13 is exactly equal to -1/2 when Leverett scaling is valid (eq. 11). However, this frequently applied relation is properly restricted to materials with a common porosity and geometrically similar pore structure (Miller & Miller, 1956).

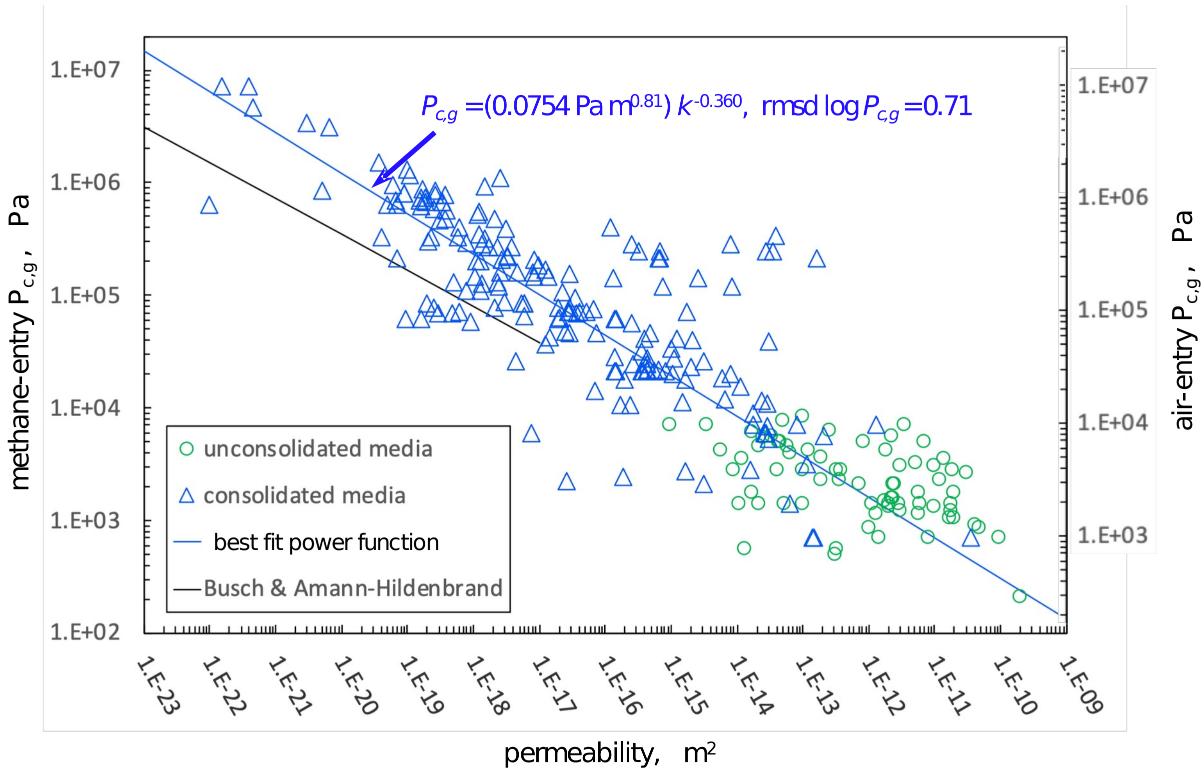

Figure 2. Correlation between gas entry $P_{c,g}$ and permeability k, for methane-water at 70 ˚C, 20 MPa (left ordinate), and for air-water at 20 ˚C, 0.1 MPa (right ordinate). The regression relation is for the methane case.

Although the Leverett *J* function contains the ratio $(k/n)^{-0.5}$, this approach is not expected to be advantageous over large variations in *n* because required geometric similitude (Miller & Miller, 1956) is not maintained. Inclusion of porosity (here, $\Delta\theta$) in scaling appears to have originated from reliance on a capillary tube bundle analogy and experimental testing over only a narrow range of *n*. The original experiments on packed sand columns by Leverett only spanned $0.39 < n < 0.49$ (Leverett, 1941). To test the utility of scaling with *n*, the $P_{c,g}$ data from Figure 2 were replotted with respect to $(k/n)^{-0.5}$ in Figure 3 (excluding a few points that lacked reported values for *n*). The best fit to Leverett scaling $(k/n)^{-0.5}$ and an empirical power function fit are included in this plot. Again, there is considerable scatter in the data, but Leverett scaling clearly performs poorly when applied over wide ranges in both *k* and *n* (rmsd $\log P_{c,g}$ = 0.76) The empirical power function depending on $(k/n)^{-0.404}$ provides a better fit, with a 0.73 rmsd for $\log P_{c,g}$.

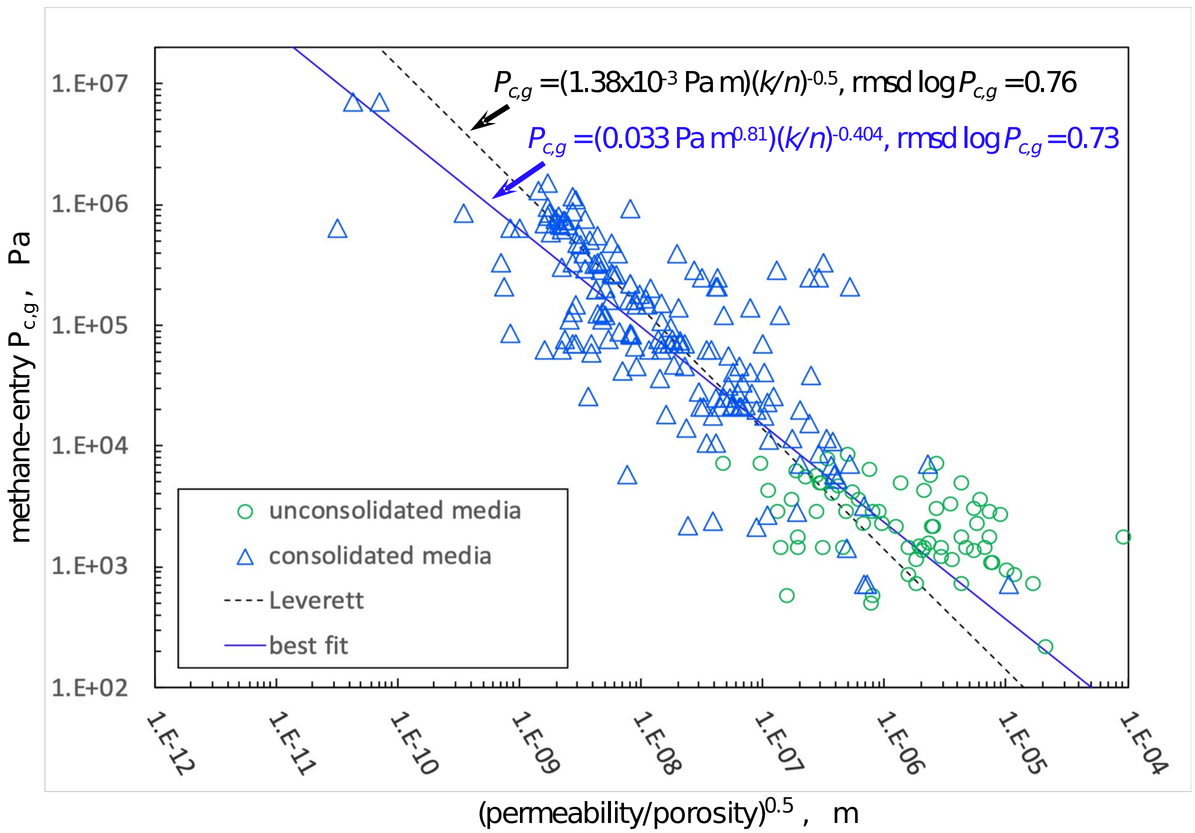

Figure 3. Correlations between $P_{c,g}$ and the square-root of k/n, showing poorer predictions based on Leverett scaling.

Although $P_{c,g}$ can now be estimated based on k, estimates of $P_{c,f}$ values are needed in order to simplify the GA imbibition equation. For this purpose, the correlation between $P_{c,g}$ and $P_{c,f}$ is next evaluated. Only a small subset of the assembled data included relations between relative permeability and P_c needed to evaluate $P_{c,f}$ using Equation 4 (Supporting Information, Table S3). Nevertheless, Figure 4 shows that the values from consolidated and unconsolidated media are highly linearly correlated over two orders of magnitude, with $P_{c,f} \approx 1.21 P_{c,g}$. Recall that this analysis is restricted to low initial moisture contents, and that higher initial saturations decrease imbibition rates.

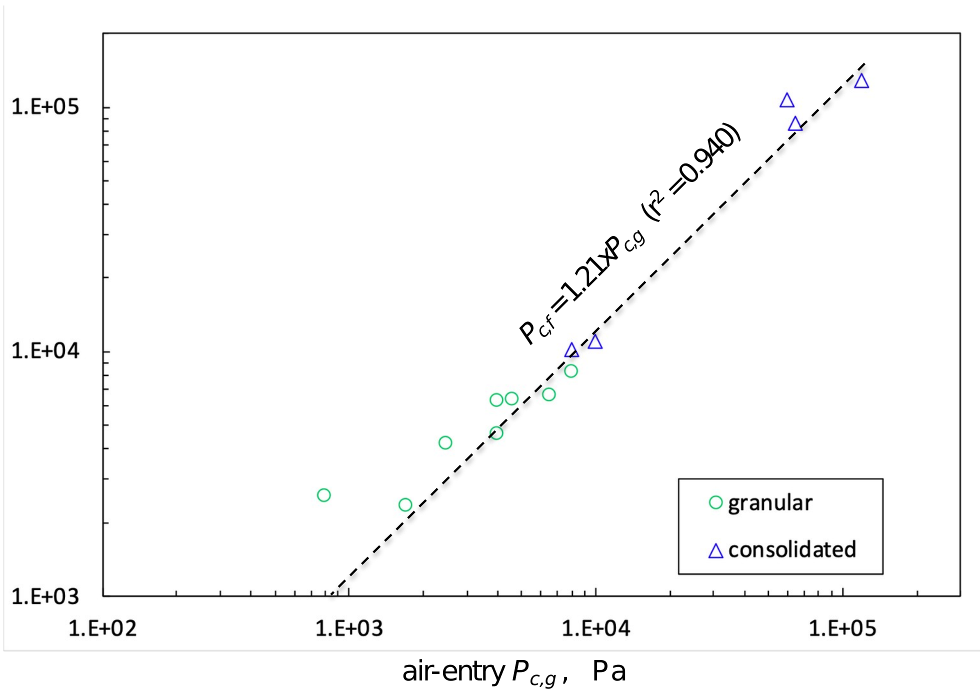

Figure 4. Correlation between P_c for air-entry and P_c at the wetting front. The highest $P_{c,f}$ values are from samples of Woodford Shale (Tokunaga et al., 2017).

Multiplying eq. 13 by 1.21 yields the relation between $P_{c,f}$ and k,

$$P_{c,f} = j_2 k^{-0.360} \tag{14}$$

where j_2 = 0.0912 Pa m$^{0.72}$. Pressurization required for hydraulic fracturing ensures that $P_{c,0} < 0$, and we assign a constant local shut-in $P_{c,0} = bP_{c,f}$ at the fracture-matrix boundary of interest, where b is negative.

5.2 Predicting wetting front advance and cumulative imbibition With these relations applied to Equations 3a and 3b, the imbibition distance and volume per unit area are approximately

$$L(t) = \left[\frac{2 j_2 (1-b)}{\eta \Delta\theta}\right]^{1/2} k^{0.32} t^{1/2} \tag{15a}$$

and

$$I(t) = \left[\left(\frac{2\Delta\theta j_2 (1-b)}{\eta}\right)^{1/2} k^{0.32}\right]^{1/2} t \tag{15b}$$

respectively. Thus, when considering imbibition under constant pressure, over a wide range of both k and n, fluxes are approximately proportional to the cube-root of k. It should be noted that when Leverett's P_c scaling proportionally with $(k/n)^{-0.5}$ is assumed, and when capillary tube analogies are used (Kao & Hunt, 1996), imbibition is predicted to be proportional to $k^{1/4}$.

5.3 Predictions of permeability based on sorptivity measurements

The various relations developed above for calculating *k* based on imbibition rates can now be tested. Recall that two of these relations were presented earlier; one developed in Tokunaga and Wan [2001] based on imbibition correlations evaluated by Kao and Hunt [1996] is eq. 9a, and the second combines the $P_{c,f}$ –*k* relation in Leverett scaling to give eq. 12. A third relation is obtained when α = -0.360 is used in the empirical relation between *k* and *S* introduced in eq. 9b,

$$k = \left(\frac{\eta}{2\, j_2 \triangle \theta} \right)^{1.56} S^{3.12} \tag{16}$$

Comparisons between measured *k* and the sorptivity-predicted *k* based on Leverett scaling of the GA model (eq. 12), the Tokunaga & Wan model (eq. 9a), and the new $P_{c,f}$ -fit GA model (eq. 16) are presented in Figure 5. It should be noted that the Leverett-scaled results were obtained by setting J = 0.0196 in eq. 12 in order to minimize the rmsd of *log k*, while no further adjustments were applied for the Tokunaga & Wan or the $P_{c,f}$-fit GA models. While all three approaches are in general agreement, predictions based on eq. 16 performed the best. It should also be noted that this analysis is not applicable for materials that are weakly wetting or hydrophobic. Although water contact angles are often used to account for wettability effects, such adjustments in scaling are qualitative because they do not satisfy requirements of geometric similitude (Tokunaga & Wan, 2013). Qualitatively, imbibition into less water-wettable materials would underestimate *k*.

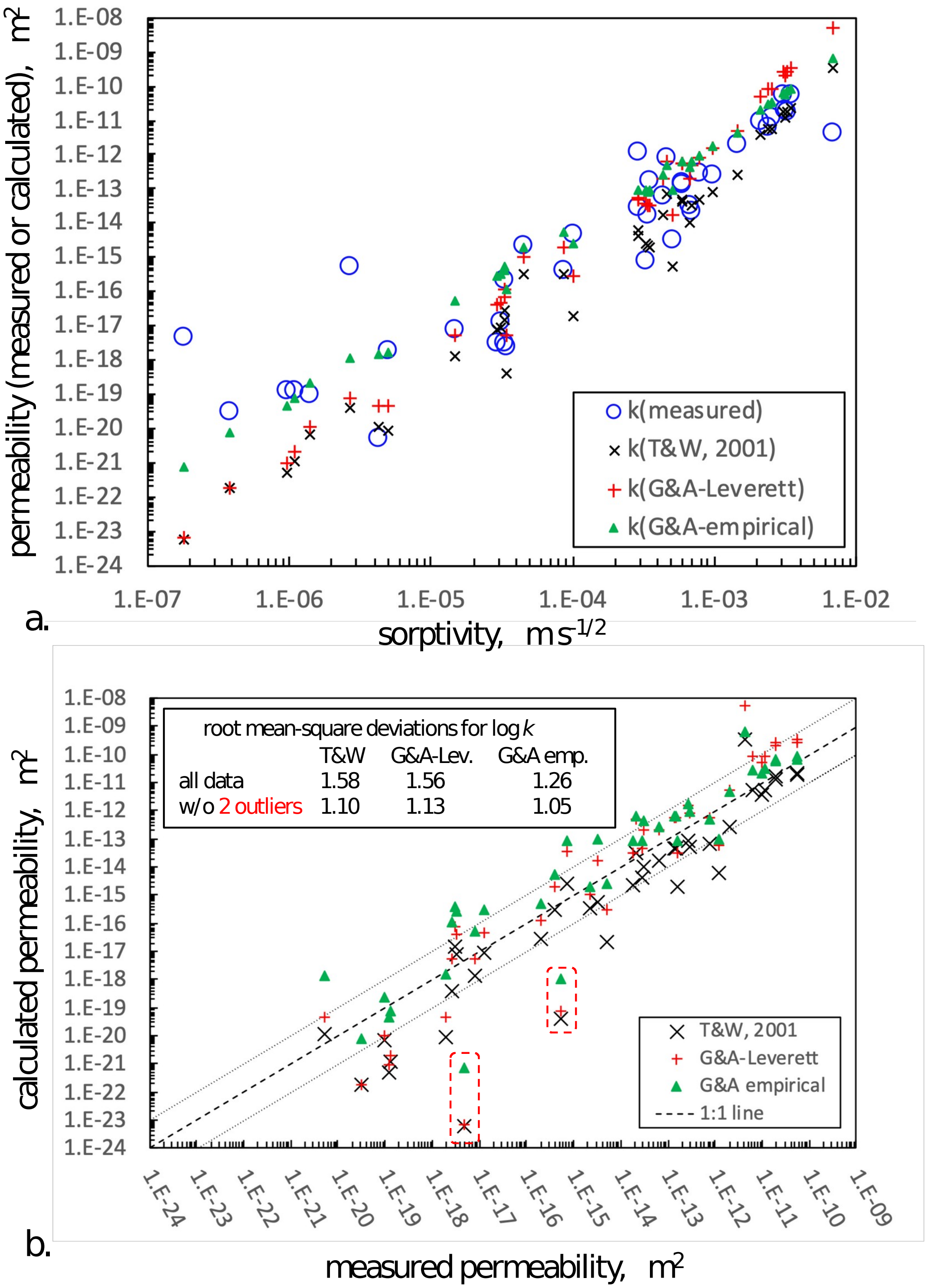

Figure 5. Estimating permeability from sorptivity. **a.** correlations between measured S and k (measured, and S-based calculated). **b.** Comparisons between measured k and k estimated based on Tokunaga and Wan (eq. 9a), Leverett-scaled GA model (eq. 12), and empirically scaled GA model (eq. 16).

The two k that significantly deviate from predictions are frame in the red-dashed rectangles.

5.4 Permeability-dependence of imbibition during hydraulic fracturing Under the high effective stresses associated with deep shale reservoirs, very high pressures act along fracture-matrix boundaries. In the following example calculations, imbibition across a hydraulic fracture-matrix interface at a depth of 2.00 km is assumed to occur under constant $P_{c,0}$ = -45 MPa estimated from the fracture gradient (Feng & Gray, 2017; Gunarathna & da Silva, 2019). It is worth noting that the large magnitude of $P_{c,0}$ dominates as the driving force for imbibition, even when the matrix has extremely low k. For $k = 10^{-21}$ m^2 (nano-darcy), $P_{c,f}$ = 3.48 MPa from eq. 14. Despite this high $P_{c,f}$, the magnitude of $P_{c,0}$ in this example comparison is nearly thirteen times greater. The dominance of $P_{c,0}$ in this hydraulic fracturing scenario is even greater in more permeable media because $P_{c,f}$ is approximately proportional to $k^{-0.36}$ (eq. 13).

The shut-in time-dependence of the water block thicknesses calculated with equation 15a are shown in Figure 6a, for k ranging from 10^{-21} m^2 up to 10^{-15} m^2 (milli-darcy), for η = 0.41 and 41 mPa s, and $\Delta\theta$ = 0.05. The two viscosity values represent water at 70 ˚C and 20 MPa, and fluid that has been thickened to achieve a 100-fold increase in viscosity relative to this reference value. The corresponding cumulative imbibition amounts for η = 0.41 and 41 mPa s are plotted on the left and right ordinates, respectively. Note from equation 15a that the wetting depth depends on the inverse square-root of viscosity, hence a 100-fold increase in η reduces L by a factor of 10. The high k values were included for completeness, but are not representative of shales. For the lower k, the water block thickness will not even extend 10 cm into the shale matrix. It should also be noted that the 1-dimensional treatment of imbibition is suitable for describing wetting in the complex fracture network only until influences of wetting front convergence become important, and that depends on the characteristic distance between fractures.

The volumetric uptake of fracturing fluid amounts to scaling down the L values in Figure 6a by a factor of $\Delta\theta$ = 0.05, and the corresponding quantities are shown in Figure 6b. Here again, comparisons are provided for water and fluid with 100-fold higher viscosity. Note that for materials with $k \leq 10^{-18}$ m^2 (μD), imbibition remains ≤ 0.3 m by day 100, even for ordinary water without increased viscosity. This is consistent with the importance of densely distributed microfracture networks in facilitating large volumes of water loss during hydraulic fracturing.

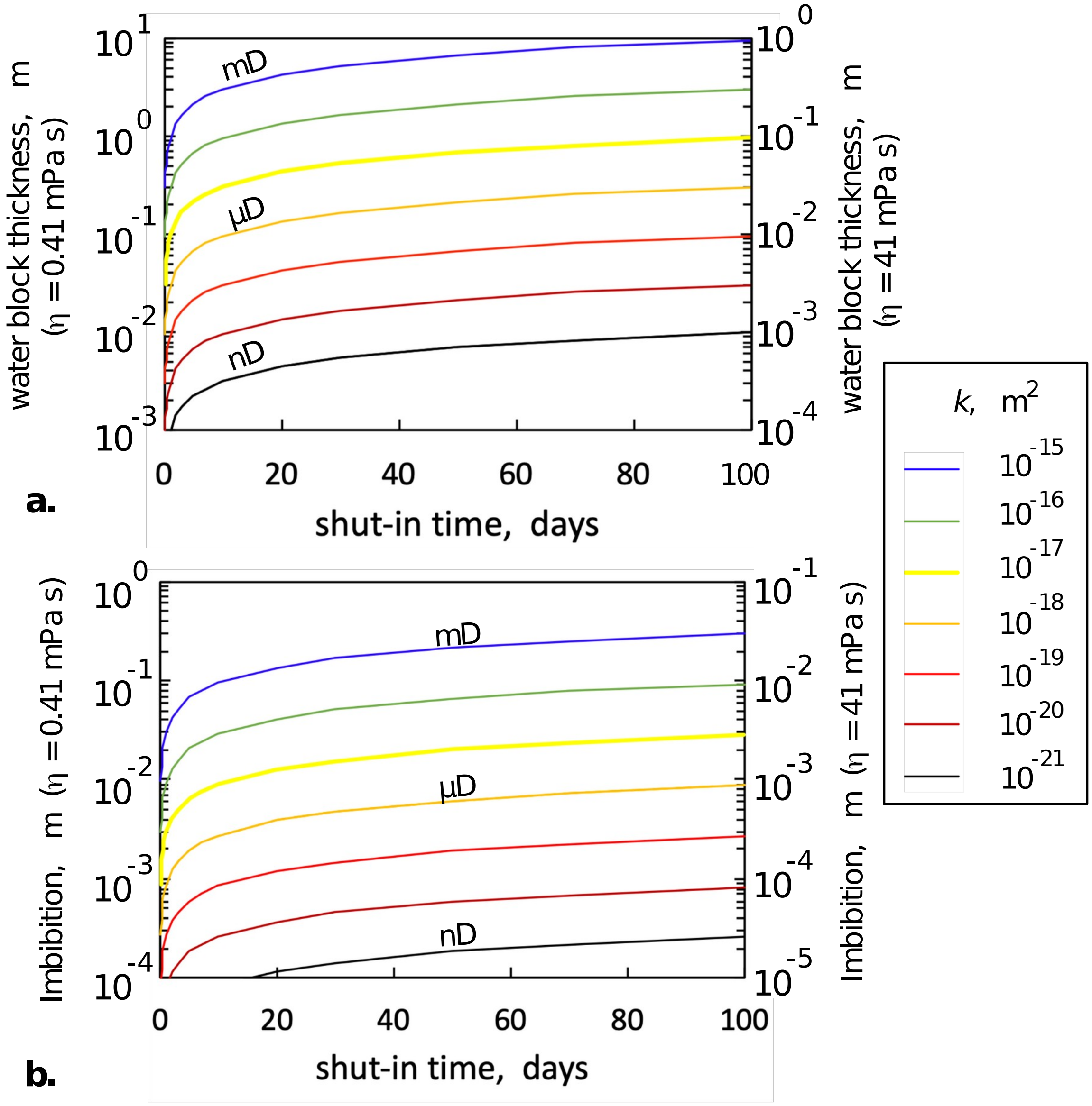

Figure 6. Time-dependence of **a.** wetting front advance (water block thickness) and **b.** cumulative water imbibition (m^3 per m^2 of fracture-shale interface area), for different matrix permeabilities. The injection pressure at the fracture-matrix boundary is 45 MPa =-$P_{c,0}$. Cases for viscosities of 0.41 and 41 mPa s correspond to the left and right ordinates of each graph.

5 Conclusions

Predicting imbibition rates and determining k are important across a wide range of disciplines. Through identifying a correlation between $P_{c,f}$ and k, results presented here facilitate predictions of both imbibition rates and k. By eliminating the need for assigning $P_{c,f}$ in the GA model, uncertainties in imbibition are largely reduced to selection of k. Conversely, results presented here show how k can be reasonably well estimated from imbibition measurements of *S*. Because of the ease with which imbibition measurements are made relative to measurements of *k*, this new approach to estimating *k* has considerable practical advantage. The G&A model modified with the $P_{c,f}$ –*k* correlation permits order of magnitude estimates of *k*, over a 10 order of magnitude range. This advantage is particularly important for measurements of low permeability materials because conventional methods are more difficult to perform and susceptible to greater experimental artifacts (Cui, Bustin, & Bustin, 2009; Tokunaga, 1988).

Given the large volumes of water consumed in hydraulic fracturing of low *k* gas reservoirs, these insights into both *k* and imbibition are relevant for understanding water loss during reservoir development. The above results facilitate calculations of local hydraulic fluid behavior at fracture-matrix boundaries, and provide predictions of the leak-off water loss rates per unit area of fracture-shale interface. Combined with information on overall leak-off losses during shut-in, these results can help estimate effective fracture-shale interfacial area within the stimulated reservoir volume. Better understanding on the dynamics of imbibition during hydraulic fracturing is a prerequisite to developing rational approached to reducing water use.

Acknowledgments

This material is based upon work supported by the U.S. Department of Energy, Office of Fossil Energy, Office of Natural Gas and Petroleum Technology, through the National Energy Technology Laboratory (NETL), under Award Number DE-AC02-05CH1123. Project management by Stephen Henry (NETL) is gratefully acknowledged. I thank John Selker, an anonymous reviewer, and Associate Editor Larry Murdoch for their insighful review comments. All data used in this paper are tabulated in the Supporting Information, and are also available in Dryad, https://doi.org/10.7941/D1V63M.

References

Agrawal, S., & Sharma, M. M. (2013). *Impact of liquid loading in hydraulic fractures on well productivity*. Paper presented at the SPE Hydraulic Fracturing Technology Conference, The Woodlands, TX.

Armitage, P. J., Faulkner, D. R., Worden, R. H., Aplin, A. C., Butcher, A. R., & Iliffe, J. (2011). Experimental measurement of, and controls on, permeability and permeability anisotropy of caprocks from the CO_2 storage project at the Krechba Field, Algeria. *Journal of Geophysical Research-Solid Earth, 116*. doi:10.1029/2011jb008385

Bell, J. M., & Cameron, F. K. (1906). The flow of liquids through capillary spaces. *Journal of Physical Chemistry, 10*(8), 658-674.

Birdsell, D. T., Rajaram, H., & Lackey, G. (2015). Imbibition of hydraulic fracturing fluids into partially saturated shale. *Water Resources Research, 51*(8), 6787-6796. doi:10.1002/2015wr017621

Bodman, G. B., & Coleman, E. A. (1944). Moisture and energy conditions during downward entry of water into soils. *Soil Science Society America Proceedings, 8*, 116-122. doi:doi:10.2136/sssaj1944.036159950008000C0021x

Bouwer, H. (1964). Unsaturated flow in ground-water hydraulics. *Journal of the Hydraulics Division, Proceedigs of the ASCE, HY5*(September), 121-144.

Busch, A., & Amann-Hildenbrand, A. (2013). Predicting capillarity of mudrocks. *Marine and Petroleum Geology, 45*, 208-223. doi:Doi 10.1016/J.Marpetgeo.2013.05.005

Byrnes, A. P., Cluff, R. M., & Webb, J. C. (2009). *Analysis of critical permeability, capillary pressure and electrical properties for Mesa Verde tight gas sandstones from Western U.S. basins* (DE-FC26-05NT42660). Retrieved from Lawrence, Kansas:

Cai, J. C., Perfect, E., Cheng, C. L., & Hu, X. Y. (2014). Generalized modeling of spontaneous imbibition based on Hagen-Poiseuille flow in tortuous capillaries with variably shaped apertures. *Langmuir, 30*(18), 5142-5151. doi:10.1021/la5007204

Chenevert, M. E. (1970). Shale alteration by water adsorption. *Journal of Petroleum Technology, 22*(Sep), 1141-1148.

Cui, X., Bustin, A. M. M., & Bustin, R. M. (2009). Measurements of gas permeability and diffusivity of tight reservoir rocks: different approaches and their applications. *Geofluids, 9*(3), 208-223.

Dehghanpour, H., Lan, Q., Saeed, Y., Fei, H., & Qi, Z. (2013). Spontaneous imbibition of brine and oil in gas shales: Effect of water adsorption and resulting microfractures. *Energy & Fuels, 27*(6), 3039-3049.

Dirksen, C. (1979). Flux-controlled sorptivity measurements to determine soil hydraulic property functions. *Soil Science Society of America Journal, 43*(5), 827-834.

Donnelly, B., Perfect, E., McKay, L. D., Lemiszki, P. J., DiStefano, V. H., Anovitz, L. M., . . . Cheng, C. L. (2016). Capillary pressure - saturation relationships for gas shales measured using a water activity meter. *Journal of Natural Gas Science and Engineering, 33*, 1342-1352.

Feng, Y. C., & Gray, K. E. (2017). Discussion on field injectivity tests during drilling. *Rock Mechanics and Rock Engineering, 50*(2), 493-498.

Gensterblum, Y., Ghanizadeh, A., Cuss, R. J., Amann-Hildenbrand, A., Krooss, B. M., Clarkson, C. R., . . . Zoback, M. D. (2015). Gas transport and storage capacity in shale gas reservoirs – A review. Part A: Transport processes. *Journal of Unconventional Oil and Gas Resources, 12*, 87-122. doi:http://dx.doi.org/10.1016/j.juogr.2015.08.001

Giesche, H. (2006). Mercury porosimetry: A general (practical) overview. *Particle & Particle Systems Characterization, 23*(1), 9-19. doi:10.1002/ppsc.200601009

Green, W. H., & Ampt, G. A. (1911). Studies on soil physics Part I - The flow of air and water through soils. *Journal of Agricultural Science, 4*, 1-24.

Gunarathna, G., & da Silva, B. G. (2019). Influence of the effective vertical stresses on hydraulic fracture initiation pressures in shale and engineered geothermal systems explorations. *Rock Mechanics and Rock Engineering, 52*(11), 4835-4853.

Handy, L. L. (1960). Determination of effective capillary pressures for porous media from imbibition data. *Transactions of the American Institute of Mining and Metallurgical Engineers, 219*(5), 75-80.

Kao, C. S., & Hunt, J. R. (1996). Prediction of wetting front movement during one-dimensional infiltration into soils. *Water Resources Research, 32*(1), 55-64. doi:Doi 10.1029/95wr02974

Katagiri, J., Saomoto, H., & Utsuno, M. (2015). Quantitative evaluation of the effect of grain aspect ratio on permeability. *Vadose Zone Journal, 14*(2).

Kondash, A. J., Lauer, N. E., & Vengosh, A. (2018). The intensification of the water footprint of hydraulic fracturing. *Science Advances, 4*(8).

Leech, C., Lockington, D., Hooton, R. D., Galloway, G., Cowin, G., & Dux, P. (2008). Validation of Mualem's conductivity model and prediction of saturated permeability from sorptivity. *ACI Materials Journal, 105*(1), 44-51.

Leverett, M. C. (1941). Capillary behavior in porous solids. *Transactions of the American Institute of Mining and Metallurgical Engineers, 142*, 152-169.

Ma, D. H., Zhang, J. B., Lu, Y. X., Wu, L. S., & Wang, Q. J. (2015). Derivation of the relationships between Green-Ampt model parameters and soil hydraulic properties.

Soil Science Society of America Journal, 79(4), 1030-1042. doi:10.2136/sssaj2014.12.0501

Makhanov, K., Habibi, A., Dehghanpour, H., & Kuru, E. (2014). Liquid uptake of gas shales: A workflow to estimate water loss during shut-in periods after fracturing operations. *Journal of Unconventional Oil and Gas Resources, 7*, 22-32.

Mason, G., & Morrow, N. R. (2013). Developments in spontaneous imbibition and possibilities for future work. *Journal of Petroleum Science and Engineering, 110*, 268-293. doi:10.1016/j.petrol.2013.08.018

Mattax, C. C., & Kyte, J. R. (1962). Imbibition oil recovery from fractured, water-drive reservoir. *Society of Petroleum Engineers Journal, 2*(2), 177-184. doi:Doi 10.2118/187-Pa

Mein, R. G., & Larson, C. L. (1973). Modeling infiltration during a steady rain. *Water Resources Research, 9*(2), 384-394. doi:DOI 10.1029/WR009i002p00384

Miller, E. E., & Miller, R. D. (1956). Physical theory for capillary flow phenomena. *Journal of Applied Physics, 4*, 324-332.

Morrow, N. R., & Mason, G. (2001). Recovery of oil by spontaneous imbibition. *Current Opinion in Colloid and Interface Science, 6*, 321-337.

Neuman, S. P. (1976). Wetting front pressure head in infiltration-model of Green and Ampt. *Water Resources Research, 12*(3), 564-566. doi:DOI 10.1029/WR012i003p00564

Philip, J. R. (1957a). The theory of infiltration, 4. Sorptivity and algebraic infiltration equations. *Soil Science, 84*, 257-264.

Philip, J. R. (1957b). The theory of infiltration: 5. The influence of the initial moisture content. *Soil Science, 84*(4), 329-340.

Rapoport, L. A. (1955). Scaling laws for use in design and operation of water-oil flow models. *Transactions of the American Institute of Mining and Metallurgical Engineers, 204*(9), 143-150.

Richards, L. A. (1931). Capillary conduction of liquids through porous mediums. *Physics-a Journal of General and Applied Physics, 1*(1), 318-333. doi:Doi 10.1063/1.1745010

Rosa, L., Rulli, M. C., Davis, K. F., & D'Odorico, P. (2018). The water-energy nexus of hydraulic fracturing: A global hydrologic analysis for shale oil and gas extraction. *Earths Future, 6*(5), 745-756.

Roychaudhuri, B., Tsotsis, T. T., & Jessen, K. (2013). An experimental investigation of spontaneous imbibition in gas shales. *Journal of Petroleum Science and Engineering, 111*, 87-97.

Sachs, W., & Meyn, V. (1995). Pressure and temperature dependence of the surface tension in the system natural gas/water. Principles of investigation and the first precise experimental data for pure methane/water at 25 0 C up to 46.8 MPa. *Colloids and Surfaces A: Physicochemical and Engineering Aspects, 94*, 291-301.

Schmid, K. S., & Geiger, S. (2012). Universal scaling of spontaneous imbibition for water-wet systems. *Water Resources Research, 48*(3), n/a-n/a. doi:10.1029/2011wr011566

Schmid, K. S., & Geiger, S. (2013). Universal scaling of spontaneous imbibition for arbitrary petrophysical properties: Water-wet and mixed-wet states and Handy's conjecture. *Journal of Petroleum Science and Engineering, 101*, 44-61. doi:10.1016/j.petrol.2012.11.015

Schmidt, K. A. G., Folas, G. K., & B., K. (2007). Calculation of the interfacial tension of the methane-water system with linear gradient theory. *Fluid Phase Equilibria, 261*, 230-237.

Schmitt, L., Forsans, T., & Santarelli, F. J. (1994). Shale Testing and Capillary Phenomena. *International Journal of Rock Mechanics and Mining Sciences & Geomechanics Abstracts, 31*(5), 411-427. doi:Doi 10.1016/0148-9062(94)90145-7

Selker, J. S., & Assouline, S. (2017). An explicit, parsimonious, and accurate estimate for ponded infiltration into soils using the Green and Ampt approach. *Water Resources Research, 53*(8), 7481-7487. doi:10.1002/2017wr021020

Stewart, R. D., Rupp, D. E., Abou Najm, M. R., & Selker, J. S. (2013). Modeling effect of initial soil moisture on sorptivity and infiltration. *Water Resources Research, 49*(10), 7037-7047.

Stukan, M. R., Ligneul, P., Crawshaw, J. P., & Boek, E. S. (2010). Spontaneous imbibition in nanopores of different roughness and wettability. *Langmuir, 26*(16), 13342-13352. doi:10.1021/la101995t

Tas, N. R., Haneveld, J., Jansen, H. V., Elwenspoek, M., & van den Berg, A. (2004). Capillary filling speed of water in nanochannels. *Applied Physics Letters, 85*(15), 3274. doi:10.1063/1.1804602

Tokunaga, T. K. (1988). Laboratory permeability errors from annular wall flow. *Soil Science Society of America Journal, 52*(1), 24-27.

Tokunaga, T. K., Shen, W. J., Wan, J. M., Kim, Y., Cihan, A., Zhang, Y. Q., & Finsterle, S. (2017). Water saturation relations and their diffusion-limited equilibration in gas shale: Implications for gas flow in unconventional reservoirs. *Water Resources Research, 53*(11), 9757-9770.

Tokunaga, T. K., & Wan, J. (2001a). Approximate boundaries between different flow regimes in fractures rocks. *Water Resources Research, 37*, 2103-2111.

Tokunaga, T. K., & Wan, J. (2001b). Surface zone flow along unsaturated rock fractures. *Water Resources Research, 37*, 287-296.

Tokunaga, T. K., & Wan, J. M. (2013). Capillary pressure and mineral wettability influences on reservoir CO_2 capacity. *Geochemistry of Geologic CO2 Sequestration, 77*, 481-503. doi:10.2138/rmg.2013.77.14

Washburn, E. W. (1921). The dynamics of capillary flow. *Physical Review, 17*(3), 273-283.

White, I., & Perroux, K. M. (1987). Use of sorptivity to determine field soil hydraulic properties. *Soil Science Society of America Journal, 51*(5), 1093-1101.

Yang, R., Guo, X. S., Yi, J. Z., Fang, Z. X., Hu, Q. H., & He, S. (2017). Spontaneous imbibition of three leading shale formations in the Middle Yangtze Platform, South China. *Energy & Fuels, 31*(7), 6903-6916. doi:10.1021/acs.energyfuels.7b00843

Zhou, Z., Abass, H., Li, X. P., & Teklu, T. (2016). Experimental investigation of the effect of imbibition on shale permeability during hydraulic fracturing. *Journal of Natural Gas Science and Engineering, 29*, 413-430. doi:10.1016/j.jngse.2016.01.023